JOURNAL OF MECHANICS OF CONTINUA AND MATHEMATICAL SCIENCES
www.journalimcms.org

ISSN (Online) : 2454 -7190 , Special Issue, No.-12, August (2025) pp 49-63 ISSN (Print) 0973-8975

THE ESIS MODEL: ENHANCED SOCIAL INFORMATION SPREAD MODEL FOR MULTI-SOURCE INFORMATION DIFFUSION IN SOCIAL NETWORKS

Shalni Chandra[1], Surjeet Singh Chauhan (Gonder)[2]

[1,2] Mathematics Department, Chandigarh University, Punjab, India-140413,

Email: [1]shalnichandra97@gmail.com, [2]surjeetschauhan@yahoo.com,

Corresponding Author: **Surjeet Singh Chauhan (Gonder)**

https://doi.org/10.26782/jmcms.spl.12/2025.08.00005

(Received: May 14, 2025; Revised: July 22, 2025; Accepted: August 05, 2025)

Abstract

In this paper, we propose a refined mathematical framework-termed the 'ESIS model', to address key limitations found in the classical SSEIR model of information propagation. Since the SSEIR model offers a foundational approach to capturing the dynamics of information spread, it falls short in representing scenarios where information circulates or stays active in a population over time. To overcome this, the ESIS model introduces a modified structure with additional compartments that more accurately represent the real-world flow of information. We develop its corresponding system of dynamic differential equations and offer a thorough state transition diagram to illustrate the behavior of individuals across different stages of information exposure. To assess the performance of the ESIS model, we simulate and compare it against the SSEIR framework through graphical analysis. The results indicate that the ESIS model enables more sustained and realistic propagation, making it a more effective tool for studying long-term influence in social networks and other information-driven systems.

Keywords: Information, model, SSEIR, active, hypergraph, Social, Susceptible.

Nomenclature

$\mathcal{W}$	Set of nodes (users) in the hypergraph.
ψ	Number of neighboring nodes (adjacency count)
$\mathfrak{m}$	Number of groups (hyperedges) formed per new node.
$\mathfrak{m}_1$	Number of existing nodes selected per group.
S_{i}	Susceptible inactive users
S_a	Susceptible active users
S_h	Highly active users.

E_1 Passively exposed.

E_2 Engaged exposed.

I_1 Informer.

I_2 Influencer.

R Recovered (no longer spreading information)

Δť Small time increment in simulations at a time ť.

de Neighbor relation function in mean-field theory

$\mathcal{P}_{S_iS_i}(\psi, ť)$ Proportion of S_i nodes with ψ neighbors at a time ť.

$\mathcal{P}_{aS_a}(\psi, ť)$ Proportion of S_a nodes with ψ neighbors at a time ť.

$\mathcal{P}_{S_hS_h}(\psi, ť)$ Proportion of S_h nodes with ψ neighbors at a time ť.

Greek Symbols

α probability of inactive users becoming active.

β probability of active user becoming highly active.

μ probability of highly active user becoming passive exposed upon contact.

η probability of highly active user becoming engaged exposed upon contact.

δ_1 probability of passive exposure stage transition to engaged exposure.

δ_2 probability of passive exposure stage transition to the Informed state.

δ_2 probability of engage exposure stage transition to the Influence state.

γ_1, γ_2 probability of users transitioning to the recovered state.

$\rho \cdot \tau \cdot c$ re-exposure probability weighted by trust τ and community factor c.

I. Introduction

Rapid growth of online social networks, such as Facebook, Twitter, and Reddit, is fundamentally changing the way information circulates amongst people and communities, since the content is received rapidly, far and wide through various channels and sources. One of the earliest and most foundational analogies was drawn by Goffman and Newill [III], who pioneered the treatment of information spread through the lens of epidemic theory, marking a turning point in how influence propagation was modeled mathematically. Over the decades, this perspective has evolved dramatically, fueled by the emergence of complex online platforms and user behaviors that are far richer and less predictable than simple contagion models could accommodate. Contemporary studies have explored this phenomenon through increasingly refined mathematical frameworks. Al-Oraiqat et al. [I] emphasized the role of strategic modeling in capturing diverse influence behaviors within social networks, showcasing how different parameters affect the reach and velocity of information dissemination. Similarly, Tong et al. [XII] introduced a fractional SEIRS model tailored for social media contexts, reflecting memory effects and delayed interactions often overlooked in classical models.

While graph-based models have formed the backbone of much of this research, a growing body of literature advocates for the use of hypergraphs to better represent higher-order relationships within networks. For example, Zhang et al.[XVII] proposed a hypergraph-based framework for influence maximization, enabling the modeling of group-level interactions rather than just pairwise links. These higher-order structures are particularly crucial in settings where information originates from communities or shared interests rather than individual nodes. Further supporting this shift, Xiao et al. [XIV] and Vasilyeva et al. [XIII] delved into hypergraph entropy and distance metrics, respectively, expanding the mathematical vocabulary available for understanding such networks. Several models have also incorporated behavioral nuances such as user competition, emotional response, or stifler dynamics. For instance, Liu et al. [IX] developed the SHIR model to analyze competing information streams, while Wang et al. [XV] proposed the ESIS model, capturing emotional feedback in spreader-ignorant-stifler dynamics. More recently, Zhu et al. [XVIII] explored how sensitive information, such as privacy-related data, disseminates across social networks, suggesting that content type significantly alters propagation patterns.

In parallel to the evolution of these models, mathematical advancements have enabled more precise control and analysis of information flow. Fixed-point theory, particularly within generalized metric frameworks, has proven useful in analyzing stability and convergence properties in these systems. Notably, Gonder et al. [IV] applied fixed-point results to graphical cone bbb-metric spaces to address complex boundary value problems, offering valuable insights into the underlying structure of dynamic systems. The integration of hypergraph structures with fixed-point techniques offers a promising frontier. Seidman [XI] laid the foundational work on hypergraph-induced social structures, which has since been extended by studies on hypernetworks and scale-free properties, as seen in the work of Hu et al. [V]. Such approaches have now been adopted to model complex user behaviors, attention shifts, and influence hierarchies in heterogeneous and dynamic networks [XVI, XIX]. Despite significant progress, current models often fail to fully capture the layered nature of influence propagation in real-world networks, particularly in scenarios involving reactivation, selective attention, and controlled spread. This paper proposes an enhanced information diffusion model that incorporates behavioral feedback loops, differentiated activity states, and a hypergraphical network representation. Building upon recent surveys and comparative evaluations [VI, VII, VII], the model generalizes existing frameworks such as SSEIR and ESIS, providing greater adaptability and realism. It aims to bridge the gap between abstract mathematical formalism and the practical complexities of online social ecosystems.

Yet, most of these models only take into consideration one source of information and rarely take into account the complexities present in the case of multiple sources of information having a simultaneous impact on user behavior. However, we propose a refined information dissemination model as an evolution of the classical SSEIR model -ESIS model, which incorporates multiple sources of information with their pathway of exposure and transmission from each source. One of the key enhancements in our model lies in distinguishing between different activity levels within the susceptible population. By introducing intermediate stages of exposure and influence, as well as

the possibility of user re-engagement, the model captures a more nuanced and realistic view of how information spreads in online environments. These refinements reflect the complexities of user behavior, where individuals may not simply adopt or reject information, but might pass through phases of passive observation, active sharing, or later reactivation. Such a detailed framework can offer deeper insights into the pathways through which content circulates across digital platforms. Ultimately, this improved modeling approach may contribute to more effective strategies for managing information flows, identifying key audience segments for outreach, and mitigating the spread of harmful or misleading content.

Limitations of the SSEIR Model:

Despite its wide use to analyze information dissemination, the SSEIR model suffers from the fact that it has limitations, which limit its application to realistic scenarios. Its skill to expand without a check on the information in unrestricted exponential bounces off over the timescale is one of the major drawbacks. In the SSEIR, once the information starts flowing, it flows at an increasing rate, and all of that is without regard to natural barriers like saturation of individuals, attention limits, or potential barriers in the population. This means that the model often has errors on the side of overestimating the spread, which is not consistent with what is observed in controlled or time-limited environments such as social networks, education systems, or strategic communication. In addition, the SSEIR model is somewhat passive as it assumes that the entire population is affected equally toward infinity with no decaying interest or information fatigue.

Proposal of the Enhanced Social Information Spread Model :

In response to key challenges observed in earlier models, we propose a refined formulation that generalizes the SSEIR framework by introducing additional behaviorally realistic features and structural dynamics. The goal is to better mirror the nature of information spread in real-world networks, where virality often reaches a peak and then stabilizes, rather than continuing unchecked. To capture this, the proposed model incorporates self-limiting mechanisms such as attention decay, selective engagement, and saturation effects, allowing the system to converge to a stable state over time that are depicted in Figure 1.

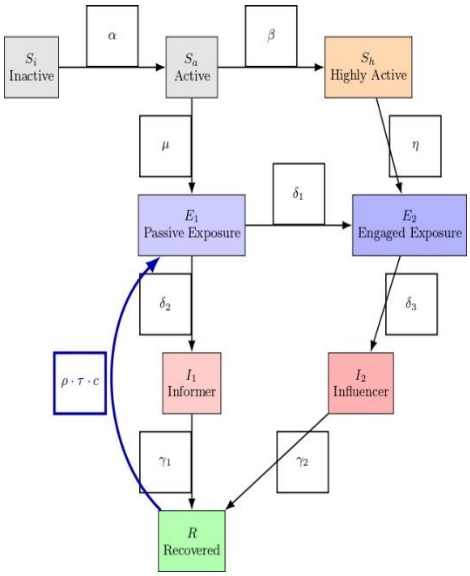

Fig. 1.

This improvement provides a framework for researching situations of controlled and sustained dissemination in addition to viral and explosive information cascades. Through its layered compartmental structure, the model captures the gradual evolution of user states across varying degrees of engagement and influence, offering more flexibility than the original SSEIR frameworks [VIII]. The updated state transition diagram (Figure X) illustrates eight distinct user compartments: inactive (S_i), active (S_a), highly active (S_h), passive exposure (E_1), engaged exposure (E_2), informer (I_1), influencer (I_2), and recovered (R). Transitions between these compartments capture the natural progression from initial exposure to becoming an active disseminator—or eventually losing interest and dropping out of the cycle. For instance, a user in the inactive state (S_i) may become active (S_a) with rate α , and subsequently progress to a highly active status (S_h) via β, depending on engagement intensity. Active users can be passively exposed (E_1) at rate μ, while highly active users may directly move to engaged exposure (E_2) via η. From these exposure compartments, individuals can transition to informer (I_1) or influencer (I_2) roles at rates δ_2 and δ_3 , respectively. Eventually, informers and influencers stop spreading and become recovered (R) through rates γ_1 and γ_2 , which represent the natural fade-out due to loss of novelty or relevance.

One of the notable extensions in our model is the re-exposure loop, where recovered individuals may return to the passive exposure class (E_1) due to renewed interactions with content shared by active nodes. This dynamic is modeled through the composite function ρ·τ·c, capturing how content re-circulation reactivates dormant users, a common feature of social media behavior. Importantly, the parameterization of our model partially builds upon values used in the original SSEIR model, particularly for the rates α, β, γ, and θ, which were derived from empirical patterns in prior studies. We preserve these foundational choices to ensure compatibility and traceability of model behavior, while extending the framework with additional states and parameters to

improve realism. To validate the robustness of our model, we conducted a sensitivity analysis by varying key parameters such as η, δ_2, δ_3, γ_1 and γ_2 across different ranges, while holding others fixed. Results demonstrate that while the quantitative magnitude of spread varies (e.g., peak values of I_2), the qualitative dynamics and convergence behavior remain consistent. This confirms that the model is not overly sensitive to small fluctuations in parameter values, supporting its suitability for varied real-world scenarios. By combining extended state modelling with grounded parameter choices and robustness testing, the proposed model offers a comprehensive and flexible tool for studying multi-source information propagation in complex networks.

This enhanced model captures more realistic dynamics of information dissemination by:

a) Differentiating between passive and active exposure,

b) Distinguishing between informers and influencers,

c) Introducing re-engagement for recovered users,

d) Recognizing varying activity levels in social behavior.

The structure and transitions in this model are visually represented in Figure 1, where each node and directional flow reflect a specific user state and its possible evolutions.

II. Mathematical Model

To examine the behavior of the proposed model and validate the theoretical formulations, a numerical simulation was carried out under a fixed set of parameter values:

Let $\mathcal{W}(\psi, \mathfrak{t})$ represent the total number of nodes connected to ψ neighbors at time $\mathfrak{t}$. Under this assumption, the following dynamics take place:

$$S_i(\psi,\mathfrak{t}) + S_a(\psi,\mathfrak{t}) + S_h(\psi,\mathfrak{t}) + E_1(\psi,\mathfrak{t}) + E_2(\psi,\mathfrak{t}) + I_1(\psi,\mathfrak{t}) + I_2(\psi,\mathfrak{t}) + R(\psi,\mathfrak{t}) = \mathcal{W}(\psi,\mathfrak{t}) \quad (1)$$

Over the time span from $\mathfrak{t}$ to $\mathfrak{t} + \Delta\mathfrak{t}$, the variation in the count of nodes within each state can be described as follows:

$$S_i \to S_i(\psi,\mathfrak{t}+\Delta\mathfrak{t}) = S_i(\psi,\mathfrak{t}) \cdot \overline{\mathcal{P}_{S_iS_i}}(\psi,\mathfrak{t}) \quad (2)$$

$$S_a \to S_a(\psi,\mathfrak{t}+\Delta\mathfrak{t}) = S_a(\psi,\mathfrak{t}) \cdot \overline{\mathcal{P}_{S_aS_a}}(\psi,\mathfrak{t}) \quad (3)$$

$$S_h \to S_h(\psi,\mathfrak{t}+\Delta\mathfrak{t}) = S_h(\psi,\mathfrak{t}) \cdot \overline{\mathcal{P}_{S_hS_h}}(\psi,\mathfrak{t}) \quad (4)$$

$$E_1 \to E_1(\psi,\mathfrak{t}+\Delta\mathfrak{t}) = E_1(\psi,\mathfrak{t}) + S_a(\psi,\mathfrak{t}) \cdot \left[1 - \overline{\mathcal{P}_{S_aS_a}}(\psi,\mathfrak{t})\right] - E_1(\psi,\mathfrak{t}) \cdot \left[\overline{\mathcal{P}_{E_1I_1}}(\psi,\mathfrak{t}) + \overline{\mathcal{P}_{E_1E_2}}(\psi,\mathfrak{t})\right] \quad (5)$$

$$E_2 \to E_2(\psi,\mathfrak{t}+\Delta\mathfrak{t}) = E_2(\psi,\mathfrak{t}) + S_h(\psi,\mathfrak{t}) \cdot \left[1 - \overline{\mathcal{P}_{S_hS_h}}(\psi,\mathfrak{t})\right] - E_1(\psi,\mathfrak{t}) \cdot \overline{\mathcal{P}_{E_1E_2}}(\psi,\mathfrak{t}) - E_2(\psi,\mathfrak{t}) . \overline{\mathcal{P}_{E_2I_2}}(\psi,\mathfrak{t}) \quad (6)$$

$$I_1 \to I_1(\psi, \mathfrak{t} + \Delta\mathfrak{t}) = I_1(\psi, \mathfrak{t}) + S_a(\psi, \mathfrak{t}) \cdot \left[1 - \overline{\mathcal{P}_{S_aS_a}}(\psi, \mathfrak{t})\right] + E_1(\psi, \mathfrak{t}) \cdot \overline{\mathcal{P}_{E_1I_1}}(\psi, \mathfrak{t}) - I_1(\psi, \mathfrak{t}) \cdot \overline{\mathcal{P}_{I_1R}}(\psi, \mathfrak{t}) \quad (7)$$

$$I_2 \to I_2(\psi, \mathfrak{t} + \Delta\mathfrak{t}) = I_2(\psi, \mathfrak{t}) + S_h(\psi, \mathfrak{t}) \cdot \left[1 - \overline{\mathcal{P}_{S_hS_h}}(\psi, \mathfrak{t})\right] + E_2(\psi, \mathfrak{t}) \cdot \overline{\mathcal{P}_{E_2I_2}}(\psi, \mathfrak{t}) - I_2(\mathcal{N}, \mathfrak{t}) \cdot \overline{\mathcal{P}_{I_2R}}(\psi, \mathfrak{t}) \quad (8)$$

$$R \to R(\psi, \mathfrak{t} + \Delta\mathfrak{t}) = R(\psi, \mathfrak{t}) + I_1(\psi, \mathfrak{t}) \cdot \overline{\mathcal{P}_{I_1R}}(\psi, \mathfrak{t}) + I_2(\psi, \mathfrak{t}) \cdot \overline{\mathcal{P}_{I_2R}}(\psi, \mathfrak{t}) + E_1(\psi, \mathfrak{t}) \cdot \overline{\mathcal{P}_{E_1R}}(\psi, \mathfrak{t}) - R(\psi, \mathfrak{t}) \cdot \overline{\mathcal{P}_{RE_1}}(\psi, \mathfrak{t}) \quad (9)$$

Where, $\overline{\mathcal{P}_{RE_1}}(\psi, \mathfrak{t}) = \rho \cdot \tau(\psi, \mathfrak{t}) \cdot c(\psi, \mathfrak{t})$ (re-exposure probability weighted by trust τ and community factor c). Here, it means recovered individuals can re-enter the exposure stage, potentially modeling fatigue recovery or re-engagement with information.

For any state, given that node $\mathfrak{i}$ at time $\mathfrak{t}$, the transition probability should sum to 1:

$$\begin{cases} \mathcal{P}^{\mathfrak{i}}{}_{S_iS_i}(\psi, \mathfrak{t}) + \mathcal{P}^{\mathfrak{i}}{}_{S_iS_a}(\psi, \mathfrak{t}) = 1 \\ \mathcal{P}^{\mathfrak{i}}{}_{S_aS_a}(\psi, \mathfrak{t}) + \mathcal{P}^{\mathfrak{i}}{}_{S_aE_1}(\psi, \mathfrak{t}) + \mathcal{P}^{\mathfrak{i}}{}_{S_aS_h}(\psi, \mathfrak{t}) = 1 \\ \mathcal{P}^{\mathfrak{i}}{}_{S_hS_h}(\psi, \mathfrak{t}) + \mathcal{P}^{\mathfrak{i}}{}_{S_hE_2}(\psi, \mathfrak{t}) = 1 \end{cases} \quad (10)$$

At time $\mathfrak{t}$, let χ_I denote the number of neighbours of node $\mathfrak{i}$ currently in the *I*-state; under this condition, the following takes place:

$$\mathcal{P}^{\mathfrak{i}}{}_{S_iS_i}(\psi, \mathfrak{t}) = (1 - \Delta\mathfrak{t} \cdot \alpha(\psi, \mathfrak{t}))^{\chi_I} \quad (11)$$

$$\psi = \mathfrak{n} \cdot \mathfrak{m}_1 \quad (12)$$

$$\langle \mathfrak{n} \rangle = \int_{\mathfrak{m}}^{\infty} \mathfrak{n} \cdot \mathcal{P}(\mathfrak{n}) d\mathfrak{n} = \mathfrak{m} \cdot \mathfrak{m}_1 \quad (13)$$

Now,

$$\alpha(\psi, \mathfrak{t}) = \sum_{\psi_1} \mathfrak{p}(\psi_1 | \psi) \cdot \mathfrak{p}^I(\psi_1, \mathfrak{t}) \quad (14)$$

$$\overline{\mathcal{P}_{S_iS_i}}(\psi, \mathfrak{t}) = [1 - \alpha \cdot \Delta\mathfrak{t} \cdot \alpha(\psi, \mathfrak{t})]^{\chi_I} = [1 - \alpha \cdot \Delta\mathfrak{t} \cdot \sum_{\mathcal{N}_1} \mathfrak{p}(\psi_1 | \psi) \cdot \mathfrak{p}^I(\psi_1, \mathfrak{t})]^{\psi} \quad (15)$$

$$\overline{\mathcal{P}_{S_aS_a}}(\psi, \mathfrak{t}) = [1 - \beta \cdot \Delta\mathfrak{t} \cdot \alpha(\psi, \mathfrak{t})]^{\chi_I} = \left[1 - \beta \cdot \Delta\mathfrak{t} \cdot \sum_{\mathcal{N}_1} \mathfrak{p}(\psi_1 | \psi) \cdot \mathfrak{p}^I(\psi_1, \mathfrak{t})\right]^{\psi} \quad (16)$$

$$\overline{\mathcal{P}_{S_hS_h}}(\psi, \mathfrak{t}) = [1 - \eta \cdot \Delta\mathfrak{t} \cdot \alpha(\psi, \mathfrak{t})]^{\chi_I} = \left[1 - \eta \cdot \Delta\mathfrak{t} \cdot \sum_{\mathcal{N}_1} \mathfrak{p}(\psi_1 | \psi) \cdot \mathfrak{p}^I(\psi_1, \mathfrak{t})\right]^{\psi} \quad (17)$$

Now, transition probability for Engaged states:

$$\mathcal{P}_{E_1 \to I_1} + \mathcal{P}_{E_1 \to E_2} + \mathcal{P}_{E_2 \to I_2} + \mathcal{P}_{E_1 \to E_1} = 1$$

Let:

- δ_1 be the probability that $E_1 \to I_1$.
- δ_2 be the probability that $E_1 \to E_2$.
- δ_3 be the probability that $E_2 \to I_2$.

$$\begin{cases} \mathcal{P}_{E_1 \to I_1} = \Delta\mathfrak{t} \cdot \delta_2 \\ \mathcal{P}_{E_1 \to E_2} = \Delta\mathfrak{t} \cdot \delta_1 \\ \mathcal{P}_{E_2 \to I_2} = \Delta\mathfrak{t} \cdot \delta_3 \end{cases} \quad (18)$$

And,

$$\mathcal{P}_{E_1 \to E_1} = 1 - \Delta\mathfrak{t} \cdot (\delta_1 + \delta_2 + \delta_3)$$

Transition probability for Informed states:

$$\mathcal{P}_{I_1 \to R} + \mathcal{P}_{I_2 \to R} + \mathcal{P}_{I_1 \to I_1} = 1$$

Let:

- γ_1 be the probability that $E_1 \to I_1$.
- γ_2 be the probability that $E_1 \to E_2$.

$$\begin{cases} \mathcal{P}_{I_1 \to R} = \Delta\mathfrak{t} \cdot \gamma_1 \\ \mathcal{P}_{I_2 \to R} = \Delta\mathfrak{t} \cdot \gamma_2 \end{cases} \quad (19)$$

And,

$$\mathcal{P}_{I_1 \to R} = 1 - \Delta\mathfrak{t} \cdot (\gamma_1 + \gamma_2)$$

Let ρ, τ, and c are parameters governing the feedback transition from Recovered nodes to Passive Exposure. Then,

$$\begin{cases} \mathcal{P}_{E_1 \to R} = \Delta\mathfrak{t} \cdot (\delta_2 + \gamma_1) \\ \mathcal{P}_{R \to E_1} = \Delta\mathfrak{t} \cdot \rho \cdot \tau \cdot c \end{cases} \quad (20)$$

Now, substituting equation (15) in equation (2),

$$S_i \to S_i(\psi, \mathfrak{t} + \Delta\mathfrak{t}) = S_i(\psi, \mathfrak{t}) \cdot \left[1 - \alpha \cdot \Delta\mathfrak{t} \cdot \sum_{\psi_1} \mathfrak{p}(\psi_1|\psi) \cdot \mathfrak{p}^I(\psi_1, \mathfrak{t})\right]^{\psi} \quad (21)$$

Substituting equation (16) in equation (3),

$$S_a \to S_a(\psi, \mathfrak{t} + \Delta\mathfrak{t}) = S_a(\psi, \mathfrak{t}) \cdot \left[1 - \beta \cdot \Delta\mathfrak{t} \cdot \sum_{\psi_1} \mathfrak{p}(\psi_1|\psi) \cdot \mathfrak{p}^I(\psi_1, \mathfrak{t})\right]^{\psi} \quad (22)$$

Substituting equation (17) in equation (4),

$$S_h(\psi, \mathfrak{t} + \Delta\mathfrak{t}) = S_h(\psi, \mathfrak{t}) \cdot \left[1 - \eta \cdot \Delta\mathfrak{t} \cdot \sum_{\psi_1} \mathfrak{p}(\psi_1|\psi) \cdot \mathfrak{p}^I(\psi_1, \mathfrak{t})\right]^{\psi} \quad (23)$$

Substituting equation (16),(18) in equation (5),

$$E_1(\psi, \mathfrak{t} + \Delta\mathfrak{t}) = E_1(\psi, \mathfrak{t}) + S_a(\psi, \mathfrak{t}) \cdot \left[1 - \overline{\mathcal{P}_{S_a S_a}}(\psi, \mathfrak{t})\right] - E_1(\psi, \mathfrak{t}) \cdot \left[\overline{\mathcal{P}_{E_1 I_1}}(\psi, \mathfrak{t}) + \overline{\mathcal{P}_{E_1 E_2}}(\psi, \mathfrak{t})\right. = E_1(\psi, \mathfrak{t}) + S_a(\psi, \mathfrak{t}) \cdot \left[1 - \left[1 - \beta \cdot \Delta\mathfrak{t} \cdot \sum_{\psi_1} \mathfrak{p}(\psi_1|\psi) \cdot \mathfrak{p}^I(\psi_1, \mathfrak{t})\right]^{\psi}\right] - E_1(\psi, \mathfrak{t}) \cdot \Delta\mathfrak{t} \cdot (\delta_2 + \delta_1) \quad (24)$$

Substituting equation (18),(17) in equation (6),

$$E_2(\psi,\mathfrak{t}+\Delta\mathfrak{t}) = E_2(\psi,\mathfrak{t}) + S_h(\psi,\mathfrak{t})\cdot\left[1-\overline{\mathcal{P}_{S_hS_h}}(\psi,\mathfrak{t})\right] - E_1(\psi,\mathfrak{t})\cdot \overline{\mathcal{P}_{E_1E_2}}(\psi,\mathfrak{t}) - E_2(\psi,\mathfrak{t}).\overline{\mathcal{P}_{E_2I_2}}(\psi,\mathfrak{t}) = E_2(\psi,\mathfrak{t}) + S_h(\psi,\mathfrak{t})\cdot\left[1-\left[1-\eta\cdot\Delta\mathfrak{t}\cdot \sum_{\psi_1}\mathfrak{p}(\psi_1|\psi)\cdot\mathfrak{p}^I(\psi_1,\mathfrak{t})\right]^{\psi}\right] - E_1(\psi,\mathfrak{t})\cdot\Delta\mathfrak{t}\cdot(\delta_3+\delta_1) \quad (25)$$

Substituting equation (16),(18),(19) in equation (7),

$$I_1(\psi,\mathfrak{t}+\Delta\mathfrak{t}) = I_1(\psi,\mathfrak{t}) + S_a(\psi,\mathfrak{t})\cdot\left[1-\overline{\mathcal{P}_{S_aS_a}}(\psi,\mathfrak{t})\right] + E_1(\psi,\mathfrak{t})\cdot \overline{\mathcal{P}_{E_1I_1}}(\psi,\mathfrak{t}) - I_1(\psi,\mathfrak{t})\cdot\overline{\mathcal{P}_{I_1R}}(\psi,\mathfrak{t}) = I_1(\psi,\mathfrak{t}) + S_a(\psi,\mathfrak{t})\cdot\left[1-\left[1-\beta\cdot\Delta\mathfrak{t}\cdot \sum_{\mathcal{N}_1}\mathfrak{p}(\psi_1|\psi)\cdot\mathfrak{p}^I(\psi_1,\mathfrak{t})\right]^{\psi}\right] + E_1(\psi,\mathfrak{t})\cdot\Delta\mathfrak{t}\cdot\delta_2 - I_1(\psi,\mathfrak{t})\cdot\Delta\mathfrak{t}\cdot\gamma_1 \quad (26)$$

Substituting equation (17),(18),(19) in equation (8),

$$I_2(\psi,\mathfrak{t}+\Delta\mathfrak{t}) = I_2(\psi,\mathfrak{t}) + S_h(\psi,\mathfrak{t})\cdot\left[1-\overline{\mathcal{P}_{S_hS_h}}(\psi,\mathfrak{t})\right] + E_2(\psi,\mathfrak{t})\cdot \overline{\mathcal{P}_{E_2I_2}}(\psi,\mathfrak{t}) - I_2(\psi,\mathfrak{t})\cdot\overline{\mathcal{P}_{I_2R}}(\psi,\mathfrak{t}) = I_2(\psi,\mathfrak{t}) + S_h(\psi,\mathfrak{t})\cdot\left[1-\left[1-\eta\cdot\Delta\mathfrak{t}\cdot \sum_{\mathcal{N}_1}\mathfrak{p}(\psi_1|\psi)\cdot\mathfrak{p}^I(\psi_1,\mathfrak{t})\right]^{\psi}\right] + E_2(\psi,\mathfrak{t})\cdot\Delta\mathfrak{t}\cdot\delta_3 - I_2(\psi,\mathfrak{t})\cdot\Delta\mathfrak{t}\cdot\gamma_2 \quad (27)$$

Substituting equations (16), (18), (19) in equation (9),

$$R(\psi,\mathfrak{t}+\Delta\mathfrak{t}) = R(\psi,\mathfrak{t}) + I_1(\psi,\mathfrak{t})\cdot\overline{\mathcal{P}_{I_1R}}(\psi,\mathfrak{t}) + I_2(\psi,\mathfrak{t})\cdot\overline{\mathcal{P}_{I_2R}}(\psi,\mathfrak{t}) + R(\psi,\mathfrak{t})\cdot \overline{\mathcal{P}_{E_1R}}(\psi,\mathfrak{t}) - R(\psi,\mathfrak{t})\cdot\overline{\mathcal{P}_{RE_1}}(\psi,\mathfrak{t}) = R(\psi,\mathfrak{t}) + I_1(\psi,\mathfrak{t})\cdot\Delta\mathfrak{t}\cdot\gamma_1 + I_2(\psi,\mathfrak{t})\cdot\Delta\mathfrak{t}\cdot\gamma_2 + E_1(\psi,\mathfrak{t})\cdot\Delta\mathfrak{t}\cdot(\delta_2+\gamma_1) - R(\psi,\mathfrak{t})\cdot\Delta\mathfrak{t}\cdot\rho\cdot\tau\cdot c \quad (28)$$

The temporal rate of change in the number of nodes over the interval $\Delta\mathfrak{t}$ can be expressed as follows:

$$\frac{S_i(\psi,\mathfrak{t}+\Delta\mathfrak{t})-S_i(\psi,\mathfrak{t})}{\mathcal{W}(\psi,\mathfrak{t})\cdot\Delta\mathfrak{t}} = \frac{\partial\mathfrak{p}^{S_i}(\psi,\mathfrak{t})}{\partial\mathfrak{t}} = -\mathfrak{p}^{S_i}(\psi,\mathfrak{t})\cdot\psi\cdot\alpha\cdot\sum_{\mathcal{N}_1}\mathfrak{p}(\psi_1|\psi)\cdot\mathfrak{p}^I(\psi_1,\mathfrak{t}) \quad (29)$$

$$\frac{S_a(\psi,\mathfrak{t}+\Delta\mathfrak{t})-S_a(\psi,\mathfrak{t})}{\mathcal{W}(\psi,\mathfrak{t})\cdot\Delta\mathfrak{t}} = \frac{\partial\mathfrak{p}^{S_a}(\psi,\mathfrak{t})}{\partial\mathfrak{t}} = -\mathfrak{p}^{S_a}(\mathcal{N}\psi,\mathfrak{t})\cdot\psi\cdot\beta\cdot\sum_{\mathcal{N}_1}\mathfrak{p}(\psi_1|\psi)\cdot\mathfrak{p}^I(\psi_1,\mathfrak{t}) \quad (30)$$

$$\frac{S_h(\psi,\mathfrak{t}+\Delta\mathfrak{t})-S_h(\psi,\mathfrak{t})}{\mathcal{W}(\psi,\mathfrak{t})\cdot\Delta\mathfrak{t}} = \frac{\partial\mathfrak{p}^{S_h}(\psi,\mathfrak{t})}{\partial\mathfrak{t}} = -\mathfrak{p}^{S_h}(\psi,\mathfrak{t})\cdot\psi\cdot\eta\cdot\sum_{\mathcal{N}_1}\mathfrak{p}(\psi_1|\mathcal{N})\cdot\mathfrak{p}^I(\psi_1,\mathfrak{t}) \quad (31)$$

$$\frac{E_1(\psi,\mathfrak{t}+\Delta\mathfrak{t})-E_1(\psi,\mathfrak{t})}{\mathcal{W}(\psi,\mathfrak{t})\cdot\Delta\mathfrak{t}} = \frac{\partial\mathfrak{p}^{E_1}(\psi,\mathfrak{t})}{\partial\mathfrak{t}} = -\mathfrak{p}^{E_1}(\psi,\mathfrak{t})\cdot(\delta_2+\delta_1) + \mathfrak{p}^{S_a}(\psi,\mathfrak{t})\cdot\psi\cdot\beta\cdot \sum_{\mathcal{N}_1}\mathfrak{p}(\psi_1|\psi)\cdot\mathfrak{p}^I(\psi_1,\mathfrak{t}) \quad (32)$$

$$\frac{E_2(\psi,\mathfrak{t}+\Delta\mathfrak{t})-E_2(\psi,\mathfrak{t})}{\mathcal{W}(\psi,\mathfrak{t})\cdot\Delta\mathfrak{t}} = \frac{\partial\mathfrak{p}^{E_2}(\psi,\mathfrak{t})}{\partial\mathfrak{t}} = -\mathfrak{p}^{E_2}(\psi,\mathfrak{t})\cdot(\delta_3+\delta_1) + \mathfrak{p}^{S_h}(\psi,\mathfrak{t})\cdot\psi\cdot\eta\cdot \sum_{\mathcal{N}_1}\mathfrak{p}(\psi_1|\psi)\cdot\mathfrak{p}^I(\psi_1,\mathfrak{t}) \quad (33)$$

$$\frac{I_1(\psi,\mathfrak{t}+\Delta\mathfrak{t})-I_1(\psi,\mathfrak{t})}{\mathcal{W}(\psi,\mathfrak{t})\cdot\Delta\mathfrak{t}} = \frac{\partial\mathfrak{p}^{I_1}(\psi,\mathfrak{t})}{\partial\mathfrak{t}} = -\mathfrak{p}^{I_1}(\psi,\mathfrak{t})\cdot\gamma_1 + \mathfrak{p}^{E_1}(\psi,\mathfrak{t})\cdot\delta_2 + \mathfrak{p}^{S_a}(\psi,\mathfrak{t})\cdot\psi\cdot\beta\cdot \sum_{\mathcal{N}_1}\mathfrak{p}(\psi_1|\psi)\cdot\mathfrak{p}^I(\psi_1,\mathfrak{t}) \quad (34)$$

$$\frac{I_2(\psi,\mathfrak{t}+\Delta\mathfrak{t})-I_2(\psi,\mathfrak{t})}{\mathcal{W}(\psi,\mathfrak{t})\cdot\Delta\mathfrak{t}} = \frac{\partial\mathfrak{p}^{I_2}(\psi,\mathfrak{t})}{\partial\mathfrak{t}} = -\mathfrak{p}^{I_2}(\psi,\mathfrak{t})\cdot\gamma_2 + \mathfrak{p}^{E_2}(\psi,\mathfrak{t})\cdot\delta_3 + \mathfrak{p}^{S_h}(\psi,\mathfrak{t})\cdot\psi\cdot\eta\cdot \sum_{\mathcal{N}_1}\mathfrak{p}(\psi_1|\psi)\cdot\mathfrak{p}^I(\psi_1,\mathfrak{t}) \quad (35)$$

$\frac{R(\psi,\mathfrak{t}+\Delta\mathfrak{t})-R(\psi,\mathfrak{t})}{\mathcal{W}(\psi,\mathfrak{t})\cdot\Delta\mathfrak{t}} = \frac{\partial \mathfrak{p}^{R}(\psi,\mathfrak{t})}{\partial\mathfrak{t}} = I_1(\psi,\mathfrak{t})\cdot\gamma_1 + I_2(\psi,\mathfrak{t})\cdot\gamma_2 + E_1(\psi,\mathfrak{t})\cdot(\delta_2+\gamma_1) - R(\psi,\mathfrak{t})\cdot\rho\cdot\tau\cdot c.$ (36)

After simplifying, we get the final differential dynamic equations for each state as:

$$\frac{dS_i}{d\mathfrak{t}} = -S_i\cdot\ \mathfrak{m}\cdot{\mathfrak{m}_1}^2\cdot\alpha\cdot de\cdot I$$

$$\frac{dS_a}{d\mathfrak{t}} = -S_a\cdot\ \mathfrak{m}\cdot{\mathfrak{m}_1}^2\cdot\beta\cdot de\cdot I$$

$$\frac{dS_h}{d\mathfrak{t}} = -S_h\cdot\ \mathfrak{m}\cdot{\mathfrak{m}_1}^2\cdot\eta\cdot de\cdot I$$

$$\frac{dE_1}{d\mathfrak{t}} = -(\delta_2+\delta_1)\cdot E_1 + S_a\cdot\ \mathfrak{m}\cdot{\mathfrak{m}_1}^2\cdot\beta\cdot de\cdot I$$

$$\frac{dE_2}{d\mathfrak{t}} = -(\delta_3+\delta_1)\cdot E_2 + S_h\cdot\ \mathfrak{m}\cdot{\mathfrak{m}_1}^2\cdot\eta\cdot de\cdot I$$

$$\frac{dI_1}{d\mathfrak{t}} = -\gamma_1\cdot I_1+\delta_2\cdot E_1 + S_a\cdot\ \mathfrak{m}\cdot{\mathfrak{m}_1}^2\cdot\beta\cdot de\cdot I$$

$$\frac{dI_2}{d\mathfrak{t}} = -\gamma_2\cdot I_2+\delta_3\cdot E_2 + S_a\cdot\ \mathfrak{m}\cdot{\mathfrak{m}_1}^2\cdot\eta\cdot de\cdot I$$

$$\frac{dR}{d\mathfrak{t}} = -\rho\cdot\tau\cdot c\cdot R + \gamma_1\cdot I_1 + \gamma_2\cdot I_2 + (\delta_2+\gamma_1)\cdot E_1$$

Equilibrium and Stability Analysis of the ESIS Model

To provide a deeper understanding of the system's long-term behavior, we perform an equilibrium and stability analysis of the ESIS model. This helps determine whether information propagation stabilizes, dies out, or recirculates in the social media ecosystem. The model consists of eight compartments representing user states in a digital network: inactive (S_i), active (S_a), highly active (S_h), passive exposure (E_1), engaged exposure (E_2), informer (I_1) influencer (I_2), and recovered (R). The full population is normalized such that:

$$S_i+S_a+S_h+E_1+E_2+I_1+I_2+\mathrm{R}=1$$

At equilibrium, all derivatives vanish. Thus, we set:

$$\frac{dS_i}{d\mathfrak{t}} = \frac{dS_a}{d\mathfrak{t}} = \ldots = \frac{dR}{d\mathfrak{t}} = 0$$

One natural equilibrium solution corresponds to the information-free (or saturation) state, where no further spread occurs:

$$E_1^* = E_2^* = I_1^* = I_2^* = 0,\ R^* = R_\infty,\ S_i^*, S_a^*, S_h^* \geq 0$$

This reflects a common scenario on social platforms where, after the peak of attention, content becomes outdated or ignored, and users gradually disengage. To evaluate the local stability of this equilibrium, we derived the Jacobian matrix of the system around this point. If all eigenvalues of the Jacobian evaluated at this equilibrium have negative

real parts, the system returns to equilibrium after small disturbances, implying local asymptotic stability. The role of re-exposure, captured by the feedback term ρ·τ·c·R, is crucial here. This mechanism allows previously disengaged users (in R) to re-enter the exposed state (E_1), reflecting real-world behavior such as retweets, algorithmic resurfacing, or trend resurgence.

Our analysis shows two distinct asymptotic regimes:

a) Stable decay (saturation equilibrium): If re-exposure is negligible or recovery dominates (i.e., ρ·τ·c ≪ γ1,γ2), the system converges to $R^* \to 1$, with no ongoing spread.

b) Persistent engagement (cyclic or endemic-like state): When reactivation exceeds decay, the model may exhibit plateaued or cyclic behavior, maintaining non-zero values of E_1, I_1, I_2 even as ŧ→∞.

This behavior mirrors real social media dynamics where older content can regain attention or go viral again due to re-sharing mechanisms, audience targeting, or periodic relevance (e.g., memes, anniversary posts). By including both saturation and sustained dynamics, the ESIS model provides a comprehensive framework for analyzing multi-source information spread in dynamic online environments.

III. Result and Discussion

Figure 2: Evolution of Information Compartments Over Time in the ESIS Model

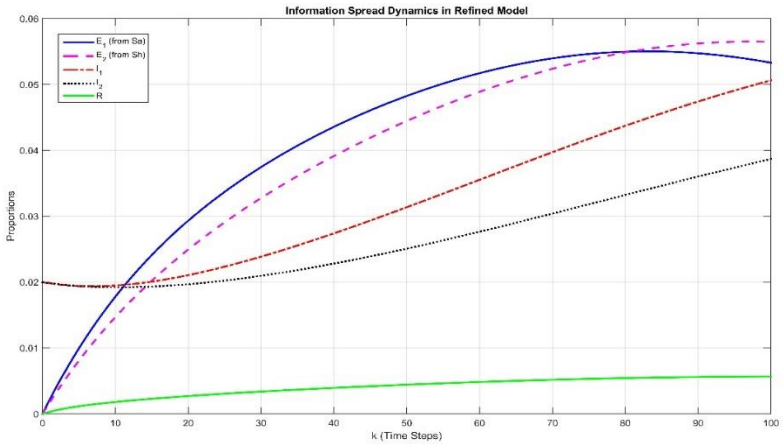

Fig. 2.

This figure illustrates the progression of key compartments in the ESIS model across discrete time steps, representing the dynamic flow of individuals through stages of exposure, influence, and recovery. The model distinguishes between two categories of exposed individuals-E_1 (from partially active users S_a) and E_2 (from highly active users S_h)-to reflect different sources of initial contact with information. Both exposure

classes increase rapidly in the early stages, with E_2 eventually surpassing E_1, indicating that high-activity sources (S_h) exert greater influence over time.

The transition into the informer class (I_1) is marked by a sharper rise, signifying rapid conversion of exposed individuals into active spreaders. The influencer class (I_2) while growing more gradually, maintains a consistent upward trend, highlighting persistent engagement and influence. The recovered compartment (R) increases slowly, suggesting that disengagement or full internalization of information is a gradual process. Overall, the figure reflects the layered and asynchronous nature of real-world information propagation, capturing how varying source types and user behaviors contribute to exposure, influence dynamics, and eventual disengagement.

Figure 3: Comparative Analysis of Active Spreaders in the SSEIR and ESIS Models

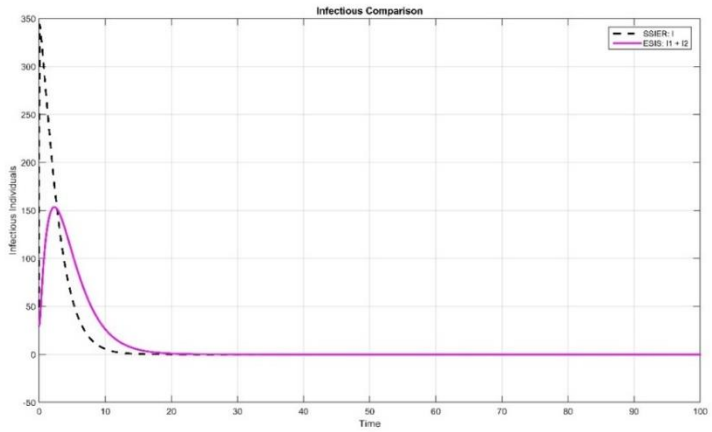

Fig. 3.

This figure compares the temporal evolution of infectious individuals in the classical SSEIR model (black dashed curve) and the proposed ESIS model (solid magenta curve) over a fixed simulation period. The SSEIR curve displays a sharp initial peak followed by a rapid decline, reflecting short-lived engagement due to the absence of sustained reactivation or influence mechanisms. In contrast, the ESIS model, which incorporates re-exposure dynamics and stratifies active users into informers (I_1) and (I_2) influencers exhibit a higher peak and a slower decay. This prolonged activity indicates extended content visibility and a more persistent propagation pattern.

The structural enhancements in the ESIS framework, especially the separation of influence roles and the modeling of re-engagement, allow it to capture realistic phenomena observed in online information ecosystems. Such dynamics include content resurfacing via sharing loops, platform-driven exposure (e.g., notifications, algorithms), and prolonged user influence. This comparison illustrates how refined compartmentalization and behaviorally inspired modeling lead to more accurate representations of long-term digital influence and information virality.

Figure 4: Comparative Sensitivity Analysis of Re-Exposure Strength and Engagement Level in the ESIS Model

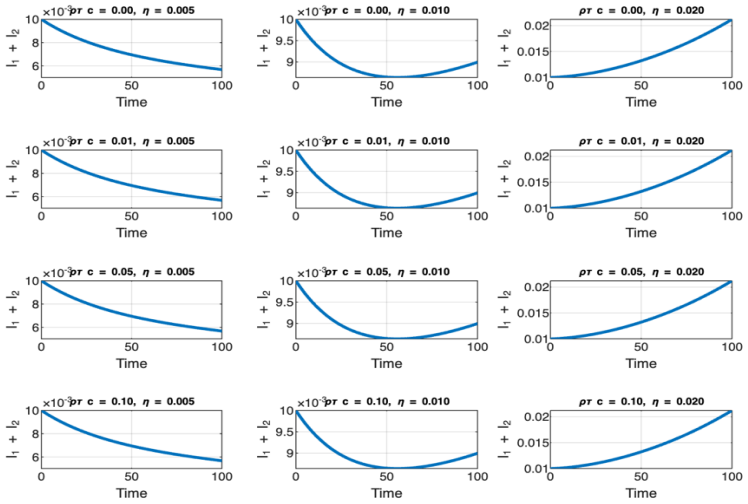

Fig. 4.

This figure displays a comprehensive sensitivity analysis of the ESIS model with respect to two key behavioral parameters: the re-exposure strength (ρ·τ·c) and the engagement level (η). The objective is to assess how variations in these parameters influence the dynamics of total active spreaders $(I_1 + I_2)$ over time. The figure comprises a grid of 12 subplots, each corresponding to a distinct parameter combination where ρ·τ·c ∈ {0,0.01,0.05,0.10} (rows) and η∈{0.005,0.010,0.020} (columns). All other model parameters were held constant to isolate the effects of these two variables.

The leftmost column highlights that lower engagement values yield slower and more prolonged information spread, whereas the rightmost column shows that higher engagement levels cause rapid but short-lived peaks in active spreaders. Similarly, increasing re-exposure strength down the rows prolongs the tail of the propagation curve, indicating sustained influence in the population. The results demonstrate the synergistic effect of re-exposure and engagement: higher values of both lead to more intense and enduring propagation, while lower values result in rapid decay. This analysis underlines the behavioral richness and adaptability of the ESIS model in capturing complex dynamics of long-term influence spread in social networks.

IV. Conclusions

For that purpose, in this study, we have developed the ESIS model as a richer model than the classical SSEIR framework for modeling the information propagation dynamics. The ESIS model takes into account more compartments and finesse the transition mechanisms, which lie more effectively in the persistence and the cyclical nature of information flow. Through dynamic differential equations and corresponding state transition diagrams, we can formulate our result more clearly in terms of

individual movement from different stages of exposure. Finally, simulation results confirm that the ESIS model provides more sustained and realistic information spread over time as compared to what would be provided by the SSEIR model. By doing so, it places ESIS as a better, more practicable means of analysing long-term effects in complex social systems, and it opens salient research applications in digital marketing, control of misinformation, or behavioral forecasting. Future work may consider the parameter estimation from real data and also extend to the hybrid flexible version with AI-driven exposure mechanisms.

Conflict of Interest:

There was no relevant conflict of interest regarding this paper.

References

I. Al-Oraiqat, Anas M., et al. "Modeling strategies for information influence dissemination in social networks." *Journal of Ambient Intelligence and Humanized Computing* 13.5 (2022): 2463-2477. 10.1007/s12652-021-03364-w

II. Dhol, B. S., Gonder, S. S. C., & Kumar, N. "Information and Communication Technology-Based Math's Education: A Systematic Review." *2023 International Conference on Advancement in Computation & Computer Technologies (InCACCT)*. IEEE, (2023): pp. 618-622 10.1109/incacct57535.2023.10141689

III. Goffman, William, and V. A. Newill. "Generalization of Epidemic Theory." *Nature*, vol. 204, no. 4955, 1964, pp. 225–228. 10.1038/204225a0

IV. Singh Chauhan, Surjeet, Shalni Chandra, and Prachi Garg. "Novel Insights Into Fixed-Point Results on Graphical Cone b b-Metric Space With Some Application to the System of Boundary Value Problems." *Mathematical Methods in the Applied Sciences* (2025). 10.1002/mma.11151

V. HU, F., LI, F., & ZHAO, H. "The research on scale-free characteristics of hypernetworks." *Scientia Sinica Physica, Mechanica & Astronomica* 47.6 (2017): 060501. 10.1360/sspma2016-00426

VI. Iamnitchi, Adriana, et al. "Modeling information diffusion in social media: data-driven observations." *Frontiers in Big Data* 6 (2023): 1135191. 10.3389/fdata.2023.1135191

VII. Li, Li, et al. "Information cascades blocking through influential nodes identification on social networks." *Journal of Ambient Intelligence and Humanized Computing* 14.6 (2023): 7519-7530. 10.1007/s12652-022-04456-x

VIII. Li, Mei, et al. "A survey on information diffusion in online social networks: Models and methods." *Information* 8.4 (2017): 118. 10.3390/info8040118

IX. Liu, Yun, et al. "SHIR competitive information diffusion model for online social media." *Physica A: Statistical Mechanics and its Applications* 461 (2016): 543-553. 10.1016/j.physa.2016.06.080

X. Rozemberczki, Benedek, Carl Allen, and Rik Sarkar. "Multi-scale attributed node embedding." *Journal of Complex Networks* 9.2 (2021): cnab014. 10.1093/comnet/cnab014

XI. Seidman, Stephen B. "Structures induced by collections of subsets: A hypergraph approach." *Mathematical Social Sciences* 1.4 (1981): 381-396. 10.1016/0165-4896(81)90016-0

XII. Tong, Qiujuan, et al. "The fractional SEIRS epidemic model for information dissemination in social networks." *Advances in Natural Computation, Fuzzy Systems and Knowledge Discovery: Volume 2*. Springer International Publishing, 2020. 10.1007/978-3-030-32591-6_30

XIII. Vasilyeva, Ekaterina, et al. "Distances in higher-order networks and the metric structure of hypergraphs." *Entropy* 25.6 (2023): 923. 10.3390/e25060923

XIV. Xiao, Hai-Bing, et al. "Information propagation in hypergraph-based social networks." *Entropy* 26.11 (2024): 957. 10.3390/e26110957

XV. Wang, Ruiheng, et al. "User identity linkage across social networks by heterogeneous graph attention network modeling." *Applied Sciences* 10.16 (2020): 5478. 10.3390/app10165478

XVI. Wang, Qiyao, et al. "ESIS: Emotion-based spreader–ignorant–stifler model for information diffusion." *Knowledge-based systems* 81 (2015): 46-55. 10.1016/j.knosys.2015.02.006

XVII. Zhang, Chuangchuang, et al. "Hypergraph-Based Influence Maximization in Online Social Networks." *Mathematics* 12.17 (2024): 2769. 10.3390/math12172769

XVIII. Zhu, Nafei, et al. "Modeling the dissemination of privacy information in online social networks." *Transactions on Emerging Telecommunications Technologies* 35.6 (2024): e4989. 10.1002/ett.4989

XIX. Zou, Xingzhu, et al. "Information Diffusion Prediction Based on Deep Attention in Heterogeneous Networks." *International Conference on Spatial Data and Intelligence*. Cham: Springer Nature Switzerland, (2022): pp. 99-112. 10.1007/978-3-031-24521-3_8